

Cell-to-cell Modelling of the inter-phase between Atrial and Sinoatrial Anisotropic Heterogeneous Nets

Gabriel López^{1,*}, Norma P. Castellanos², Rafael Godínez²

1 Mathematics Department, Universidad Autónoma Metropolitana, México City, México.

2 Electric Engineering Department, Universidad Autónoma Metropolitana, México City, México.

* gabl@xanum.uam.mx

Abstract

The transition between Sinoatrial cells and Atrial cells in the Heart is not fully understood. This paper focus in cell-to-cell mathematical models involving typical Sinoatrial cells and Atrial cells connected with experimentally observed conductance values exclusively. We are interested mainly in the geometry of the microstructure of the conduction paths in the Sinoatrial Node. We show with some models that appropriate source-sink relationships between Atrial and Sinoatrial cells may occur according to certain geometric arrangements.

Author Summary

In [13] Inada et al. modeled the inter-phase in a series of 200 cells, the first 50 SA, where there is a gradient in the conductance of the Ionic currents inside the cells and also a gradient in the the membrane capacitance of SA Kurata et al. cell model (see references within [13]). In that model there is also a gradient in the conductance between SA cells varying from $g_{SA} = 20$ nS to 3999.8 nS, this last value, as the authors mention, is not actually observed experimentally. For the Atrial cells they used the model of Lindblad et al. [16] with conductance between atrial cells $g_A = 4000$ nS (neither observed experimentally). In that series model the inter-phase between A and SA cells is attained by one SA cell (the 50th cell in a line) connected to three branches of 50 A cells each. The inter-phase is achieved connecting the 50th SA cell with the 49th SA cell throughout $g_{SA} = 3999.8$ nS, and connecting the 50th SA cell with three A cells with $g_{SA-A} = 4000$ nS. The conductance between A cells is kept constant $g_A = 4000$ nS. This kind of manipulation of parameters existing in the literature over the years is not allowed in our study. In the present paper g_{SA} takes values between .6 nS and 20 nS [30]. Is worth to remark that in our simulations conduction occurs with g_{SA-A} as low as .6 nS. With this parameter values we obtain appropriate source-sink relationships between Atrial and Sinoatrial cells through certain geometric arrangements.

Introduction

It has been observed in different species that going from the center of the sinoatrial node (SAN) in the heart toward the atrium, there is a transitional zone of cells having morphological and electrophysiological properties in-between to that of typical sinoatrial

(SA) and atrial (A) cells [18]. The transitional cells have an aspect intermediate between that of typical nodal cells and that of the common atrial cells. Typical nodal cells have poor development of the contractile system and is assumed in general that they do not contract, moreover the existence of connexin43 is undetectable in the SA node center (see [4] and references therein), but posses automaticity in firing its action potential. On the contrary, atrial cells do contract themselves, but they require of an stimulus in order to contract, and they contain mainly connexin-43. This characteristics are included in the cells models used in this paper. A whole range of intermediate cells have been reported, but more important to the models in this paper, cells with one end connected to SA cells and the other end with A cells have been found [18]. The basic structure conforming the cytoarchitecture of this groups of cells consists of interdigitations of nodal and atrial bundles forming histological connections between nodal and atrial myocytes at regular distances [20].

In [32] the authors, introduce a model of strands of atrial cells penetrating the SA node observed in the Pig. The model was constructed with 101×101 atrial and SA cells modeled with Oxsoft HEART V4.5. The lattice so constructed has a center of SA cells forming a circle of 30 cells of radius with twelve atrial interdigitations positioned at 30 deg intervals, where interdigitations are defined as sets of atrial cells at least ten cells distant from the node centre, and which are subtended by an angle of 15 deg. In that paper SA to SA conductance is $g_{SA} = 10$ nS and the A to A conductance g_A , varies from 10 nS to 250 nS.

With respect to the action potential model's shapes, years ago, Joyner and van Capelle [15] noticed that the presence of electrical coupling among cells create transitional action potential shapes in cells near the border zone between two distinct different cell types and that the electrotonic influences make it very difficult to prove that cells in a particular region are truly transitional in terms of their intrinsic membrane properties. Accordingly with this, in our models, action potential shapes behave in some kind of transitional manner which may provide some coincidence with the behavior of transitional cells observed in vivo. We achieve this "transitional cells" through the cytoarchitecture in the model keeping the conductance as mentioned above, i.e., without any gradient between cells.

More recently in [6], Csepe et al. study the functional-structural connection between the SAN and the atria. Their studies suggest that the microstructure of the connection paths between A and SA cells plays a crucial role in human SAN conduction and contributes to normal SAN pacemaking. Our paper may be consider as a local approach to the complexity of the specialized branching myofiber tracts comprising the SA connection paths described by Csepe et al.

Materials and Methods

In this paper we use the Lugo et al. (LC), [17] (Human) model which is a refinement of Nygren et al. (N), [19] (Human) model and, basically, modifies the dynamics of the RyR2 and Ca^{++} release of the sarcoplasmic reticulum (SR) in order to model the effect of SR release refractoriness in appearance of electromechanical alternants. The N model reconstructs action potential data that are representative of recordings from human cells. In the N model the sustained outward K^+ current determines the duration of the AP. On the other hand, the AP shape during the peak and plateau phases is determined primary by transient outward K^+ current, I_{sus} , and L-type Ca^{2+} current.

For SA cells, in our net models, we use the Severi et al. model (S), [25] (Rabbit). This model based on up-to-date experimental data, generate Action Potential (AP) waveforms typical of rabbit SAN cells whose parameters fall within experimental ranges: 352 ms cycle length, 89 mV AP amplitude, -58 mV maximum diastolic potential, 108

ms Action Potential Duration at its half amplitude (APD_{50}), and 7.1 V/s maximum upstroke velocity; and, more interesting, describes satisfactorily experimental data concerning autonomic stimulation, funny-channel blockade and inhibition of the Ca^{2+} -related system by BAPTA.

The equations used in this paper are of the form

$$\begin{aligned}\frac{dV}{dt} &= I(V) + (g_1 M_1 + g_2 M_2 + g_3 M_3 + g_4 M_4) V \\ V|_{t=0} &= V_0,\end{aligned}\tag{1}$$

where the transposed vector $V^t = (V_{A1}, \dots, V_{An}, V_{SA1}, \dots, V_{SAm})$ corresponds to the Voltage of the A (A1 to An) and SA (SA1 to SAm) cells, with n, m values varying in different models, $I(V)^t = (I(V_{A1}), \dots, I(V_{SAm}))$, is a vector representing the currents of A and SA cells, M_1 is a connection matrix between A cells, M_2 is a connection matrix between A and SA cells, M_3 gives the connections between SA and A cells, and M_4 is the connection matrix between SA cells; the constants $g_1 = g_{A-A}/C_{mA}$, $g_2 = g_{A-SA}/C_{mA}$, $g_3 = g_{SA-A}/C_{mSA}$, $g_4 = g_{SA-SA}$. Here $C_{mSA} = .000032 \mu F$; $C_{mA} = .00005 \mu F$, and g_{SA-A} , g_{A-SA} , g_{A-A} are the conductance values between corresponding cells which values are specified in each model. The vector $V|_{t=0} = V_0$, i. e. V at time $t = 0$, takes values which vary randomly with normal distributions, accordingly: for Atrial cells, mean -74.2525 mV, and for SA cells, mean -58mV, with standard variation .1 mV in both cells types. In tree models we keep $g_{SA-A} = g_{A-SA} \approx .6$ nS, with the precise value given in the corresponding model. We explore in section Series models analysis the possibility of $g_{SA-A} \neq g_{A-SA}$, which can not be excluded a priori due to the possibility of existence of different kind of connexin types in the cell-to-cell connections through the transitional zone.

We assume in our models that SA cells are synchronized in phase, as theoretically predicted in the well known paper of Torre [28]. In fact, for the S model, varying randomly V_0 in each simulation (up to 20 simulations), we obtained synchronization in phase of up to 100 SA cells, even before the first cycle ended with conductance g_{SA-SA} as low as .6 nS. For the numerical simulations of the synchronization of SA cells we considered different geometric arrangements: in series, forming an anullus, and even with a random matrix of connections (which is histologically improbable). To model connections between 100 SA cells we take in equation (1) $M_1 = M_2 = M_3 = \mathbf{0}_{100 \times 100}$ where $\mathbf{0}_{100 \times 100}$ is the zero matrix of size 100×100 , and $g_4 = .6 \text{ nS} / C_{mSA}$.

Results

We found that there exist a correspondence between supercritical Andronov-Hopf bifurcation parameters and the geometric structure of the transitional zone in the SAN, structure which coincides, at least locally, with interdigitating bundles formed by A and SA cells. These interdigitations were observed and studied in papers such as [6]. The correspondence that we found has been unnoticed in a large number of papers, leading to erroneous simulations of certain biological observations.

Cell-to-cell modeling

The cell-to-cell approach requires: a) individual cell dynamics, modeled by Hodgking-Huxley type equations. In this paper for SA node cells, we use the model of Severi et al. [25], described in section Atrial and Sinoatrial cell models, and Lugo et al.

model [17] for atrial cells; b) SA cytoarchitecture, in this paper we assume that the SA cells ran parallel and meet mostly end to end [26], and that each cell is connected via intercalated disks with approximately 9.1 ± 2.2 other cells [12]. A model of idealized two-dimensional arranges of cells using a similar structure can be found in [27]; c) In order to implement the solvers an approximate number of cells in SA node is required. This number may be estimated to be in the order of millions. In the present study our approach to the transitional zone is local and the number of cells considered, varies between 30 and 78, which is enough to approximate some source-sink relations between A and SA cells in this specific part of the SAN.

Concerning to the cytoarchitecture of SA node is important not only the number of cells to which each cell is connected (already cited) but the geometric distribution of each connection. Here we should to remark that due to the use of connections matrices for the models of this paper, the inherent three dimensionality of the cytoarchitecture (see [6] where the necessity of the 3D approach in order to understand the human SA node structure is amply discussed) does not require an special treatment as is the case for PDE, in which a tensor is required to describe the complex geometry distribution of cells in the heart [9], [10], [11], [23].

In some models we keep $g_{SA-A} = g_{A-SA} \approx .6$ nS, with the precise value given in the corresponding model. We explore in the section Series models analysis the possibility of $g_{SA-A} \neq g_{A-SA}$ existing in series models, possibility which can not be excluded a priori due to the probable of existence of different kind of connexin types in the cell-to-cell connections through the transitional zone.

Atrial and Sinoatrial cell models

There are many Atrial cell models in the literature, among them: Courtemanche et al. (CRN), [5] (Human); (RNC), [24] (Canine); Nygren et al. (N), [19] (Human); Lindblad et al. (L), [16] (Rabbit), and a more recent model of Lugo et al. (LC), [17] (Human). A comparison between the models CRN, RNC, and N can be found in [7]. In this paper we use the LC model which is a refinement of N model and, basically, modifies the dynamics of the RyR2 and CA++ release of the sarcoplasmic reticulum (SR) in order to model the effect of SR release refractoriness in appearance of electromechanical alternants. The N model reconstructs action potential data that are representative of recordings from human cells. In this model the sustained outward K^+ current determines the duration of the AP. On the other hand, the AP shape during the peak and plateau phases is determined primary by transient outward K^+ current, I_{sus} , and L-type Ca^{2+} current.

For SA cells, in our net models, we use the Severi et al. model (S), [25] (Rabbit). This model based on up-to-date experimental data, generate Action Potential (AP) waveforms typical of rabbit SAN cells whose parameters fall within experimental ranges: 352 ms cycle length, 89 mV AP amplitude, -58 mV maximum diastolic potential, 108 ms Action Potential Duration at its half amplitude (APD_{50}), and 7.1 V/s maximum upstroke velocity; and, more interesting, describes satisfactorily experimental data concerning autonomic stimulation, funny-channel blockade and inhibition of the Ca^{2+} -related system by BAPTA.

Series models

In [13] the authors modeled the inter-phase in a series of 200 cells, the first 50 SA, where there is a gradient in the conductance of the Ionic currents inside the cells and also a gradient in the the membrane capacitance of SA Kurata et al. cell model (see references within [13]). In that model there is also a gradient in the conductance between SA cells varying from $g_{SA} = 20$ nS to 3999.8 nS, this last value, as the authors

mention, exceed by far experimental values. In [13] Atrial cells are modeled with Lindblad et al. [16] with $g_A = 4000$ nS (neither observed experimentally). In that 1D model the inter-phase is attained by one SA cell (the 50th cell in a line) connected to three branches of 50 A cells each. In that model the inter-phase is achieved connecting the 50th SA cell with the 49th SA cell throughout $g_{SA} = 3999.8$ nS, and connecting the 50th SA cell with three A cells with $g_{SA-A} = 4000$ nS. The conductance between A cells is kept constant $g_A = 4000$ nS.

In [21] Oren and Clancy, study a series model (among others models) of 60 cells. In this model a gradient in coupling, shifts the site of pace maker initiation towards the periphery of SA node, a result which, as the authors mention, is not consistent with experimental observations.

As we mention in section Materials and Methods SA cells are synchronized in phase, as theoretically predicted in the well known paper of Torre [28], and as we obtained accordingly, synchronization in phase of S model. Hence, in a series model (see Fig. 1) the transition zone of the SAN can be modeled locally with just one SA cell using the S model for SA cells. We are interested in modeling without introducing coupling parameters not observed experimentally, so we keep in our simulations, SA coupling values between .6 and 25 nS [30] (Rabbit).

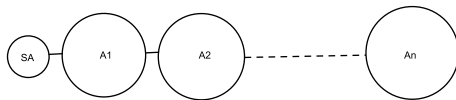


Fig 1. Series arrangement of cells.

For this model equation (1) becomes simply

$$\begin{aligned} \frac{dV}{dt} &= I(V) + (g_1 M_1 + g_3 M_3)V \\ V|_{t=0} &= V_0, \end{aligned} \quad (2)$$

where M_1 is a tridiagonal matrix with main diagonal $(-2, -2, \dots, -2)$ and sub and super diagonals $(1, \dots, 1)$; and M_3 is the matrix with first row $(-1, 0, \dots, 0, 1)$, last row $(1, 0, \dots, 0, -1)$, and an zero matrix in between this two rows.

Series models analysis

Using the N model, conduction occurs if, for instance $g_{A-SA} = g_{SA-A} = 6$ nS. We observe nevertheless, that conduction occurs if $g_{A-SA} \neq g_{SA-A}$, for instance, if g_{A-SA} is 10 fold $g_{SA-A} = 6$ nS. Curiously, the A cells AP profile behave as SA cells AP profile if $g_{A-SA} = 100g_{SA-A} = 100 \times .006$ nS.

We call selective diffusion to the phenomenon occurring in simulations in which conduction is achieved if $g_{A-SA} \neq g_{SA-A}$. The question here is if this kind of selective diffusion may actually occur in real cells, to the best of our knowledge this is an open question to date, the mechanisms of coupling mechanisms remain poorly understood. Recent studies [2] indicate that connexins as Cx43 may exert different functions besides

gap junctions formation, including non-cannonical functions in the function of sodium channel. So to-date the possibility of selective diffusion can not be excluded a priori.

Another form in which conduction fails occurs when some of the cells do not reach threshold for instance in a model with $.4g_{A-SA} = .1g_{SA-A}$.

A more interesting model is obtained if we abandon the one dimensional restriction of the series, for instance, when six or seven SA cells are attached to a series of A cells as shown in Fig 2. This models contradict the claim of Inada et al. [13] that suggest that a gradient in both electrical coupling and cell type is necessary for the SAN to drive the atrial muscle. The left hand side plot in Fig 2 shows one of seven SA cells (the first) connected in a series with atrial cells, with same conductance $g_{SAA} = g_{AA} = 6nS$. Note nevertheless, that the action potential of the first four atrial cells show a transitory cell profile, this cells are typical A cells without any gradient, so that conduction is possible. This phenomenon may explain why in vivo there appear AP of transitional cells similar to the AP of atrial cells.

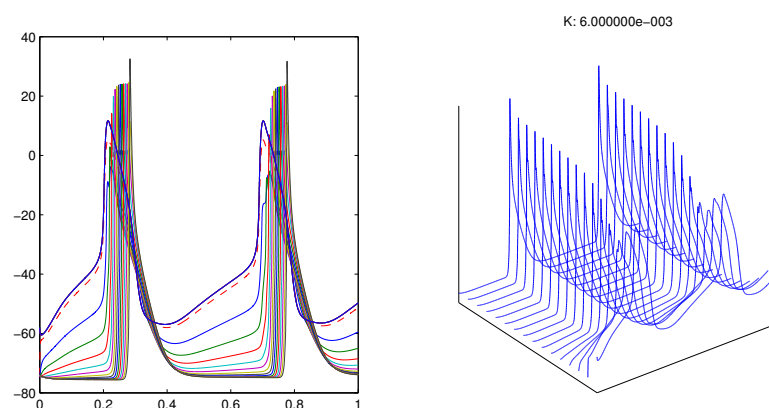


Fig 2. A series model in which conduction occurs. In the left panel V vs. t is plotted. The right panel shows the cells display as a series, in this plot only the first cell corresponds to an SA cell. The K value corresponds to the capacitance g_{SA-A} .

Conduction is not achieved

In the next section we will study models beyond series arrangements. As an introduction, we mention that if a series is divided in order to branch, then seven SA cells are not enough to propagate the AP. Accordingly, we constructed two models in which propagation fails. In the first model an A cell is connected to seven SA cell and to two A cells which in turn are connected to two disconnected series, to illustrate this, in Fig. 3, A1 is connected to A2 and to A25; A2 is connected to a series from A3 to A24; and A25, in turn, is connected to a series from A26 to A50.

The way in which conduction fails is shown in figure 4. In the second model in which conduction fails A1 is connected to seven SA cells and to A2 cell, then A2 branches into two disconnected series. The important issue here is that conduction occurs if we abandon the series model.

In fact, in figure 5 the same bifurcate series conducts AP as long as 4 SA cells are connected to each A2 and A25 cells.

The scheme of the conducting bifurcating series is shown in figure 6. Note that we only plot one SA cell, the series A2 to A14, and cells A23, A24. In the left panel only one SA cell appears, the series A2 to A14, and cells A23, A24. Observe that the

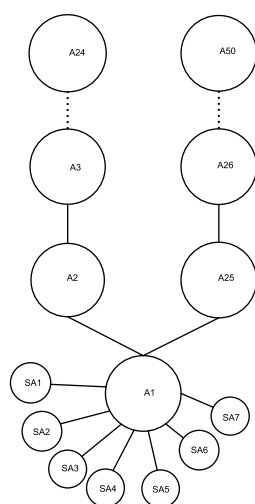


Fig 3. Two disconnected series in which conduction does not occur.

Schematic figure in which two series of A cells are connected to an A cell connected in turn with 7 SA cells. In this model conduction fails.

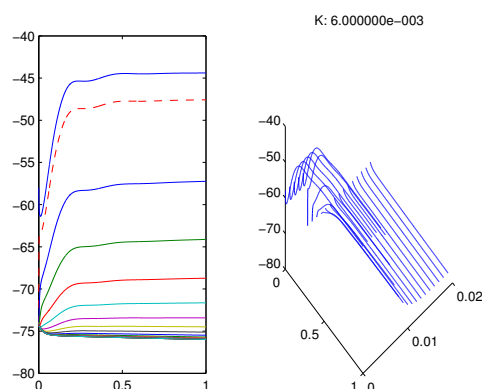


Fig 4. Series model in which conduction fails.

representation in Fig. 6 is schematic: the contact between A cells occur in vivo through discs in the extreme of cells (Atrial cells are mostly cylindrical in shape), or side to side.

Tree Net Models

We call a Tree Net a model in which each cell is connected with two or three other cells forming branches. In Tree net models the number of cell connected spreads rapidly. For instance in the tree model in which each cell is connected with three other cells, after twenty steams we would have $(3^{21}-1)/2 = 5.2e+9$ cells connected and activated by one single SA cell, a number much larger than the entire number of cells in the entire heart (the number of cells in a healthy human heart is about 2 billion ($2e+9$), [1]). Therefore, the Tree Net Model is somehow an unrealistic model for the bundle formed by SA node and Atrial cells, nevertheless, as a first approximation, it will provide some interesting information. We clarify this point, in order that an small SA node paces the heart it

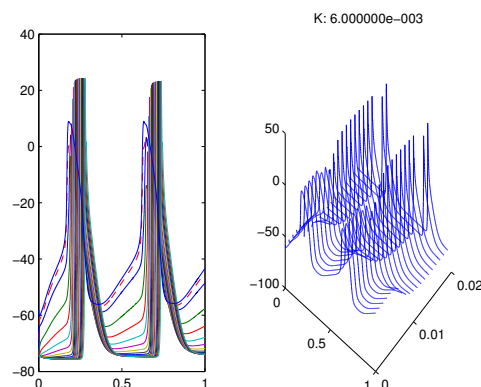


Fig 5. A bifurcated series which conducts AP. With cells connected as in Fig. 6 conduction occurs with $g_{SA-A} = g_{SA-SA}$.

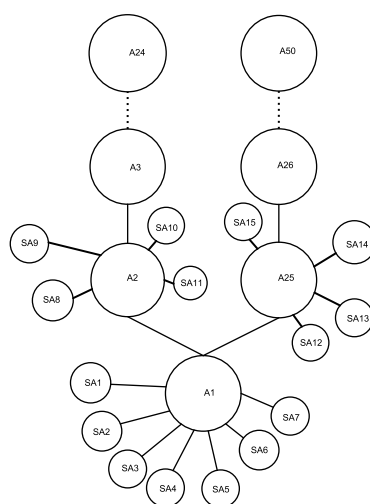


Fig 6. Two disconnected series in which conduction does occur.

should be expected that A cells do ramify, but not at every cell with disconnected branches, the manner in which Atrial cells do ramify is, to the best of our knowledge, unknown, but certainly ramifications do no occur at each cell. Nevertheless in modeling the transition between SA and A cell we found that each ramification requires a minimum number of SA cells in order to drive a tree of A cells if we want to keep g_{SA-A} within experimental values and even, if we want to keep this parameter value constant. In Fig. 7 a tree with bifurcating branches in each node of atrial cells is represented. In the figure, to illustrate a ramification we represented it schematically with two lines departing from the same point.

In Fig. 8, a tree like that in Fig. 7 i. e. with ramifications in each node is paced if A1 is connected with seven SA cells and cells A2, A3 are connected with another four SA cells each. The point here is that this net illustrates the fact that bifurcation parameters are non linear, so that when propagation of the AP is achieved the net supports some number of new ramified nodes, regardless the extra load that each ramification implies in the entire net.

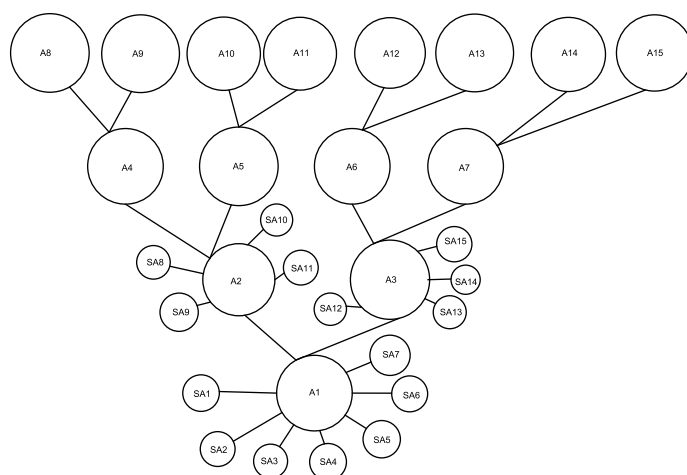


Fig 7. Tree with two-type ramifications.

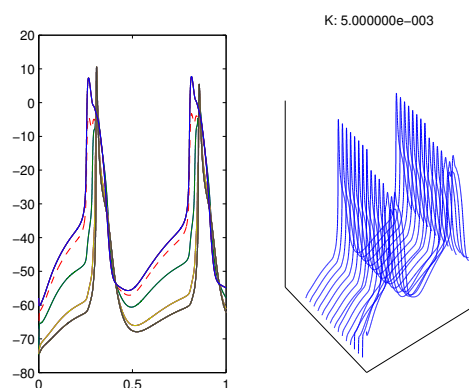


Fig 8. Conduction is achieved. If in a tree like that in Fig 7 is connected to 15 SA cells properly distributed, conduction is achieved.

A comment is worth here, clearly seven cells connected with only one cell (as in figure 6) is impossible in one dimensional series models and very difficult even in two dimensional models given SA and A cells sizes, but this number of connections may occur in three dimensional models without geometrical complications, as actually they do happen. So our model is intrinsically a model in three dimensions. But more importantly our model suggest that in order to obtain conduction with $g_{SA-A} = .5$ nS constant, the branch must be connected to a minimum number of SA cells which in our model is 15 at the first branch in a tree. Actually we have to mention that is possible to pace the net with 15 SA cells connected with A1 cell and this cell connected with a net of A cells, but we obtain subthreshold behavior in A cells, even with $g_{SA-A} = 0.57$ nS, which clearly indicates that the geometry of the net is extremely relevant (see Fig. 9) for conduction.

Finally, in numerical simulations we obtain that conduction is possible if we allow $g_{SA-A} \neq g_{A-SA}$ as in series models. In Fig. 10, $g_{A-A} = g_{SA-A} = .6$ nS, but

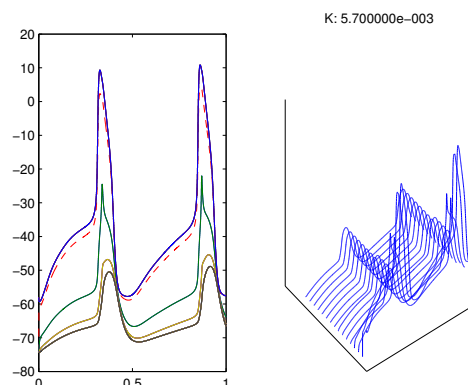


Fig 9. Tree with two-ramifications and subthreshold A cells.

$g_{A-SA} = 14$ nS. Notice that A2, A3 cells present two peaks which may be consider as an anomalous behavior.

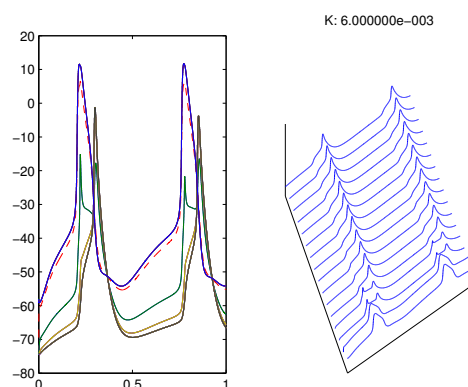


Fig 10. Tree with $g_{SA-A} \neq g_{A-SA}$.

Mathematically, at least qualitatively, the behavior of the nets of this section can be described by the existence of a supercritical Andronov-Hopf bifurcation [14], i. e., a bifurcation of an equilibrium state (sink, due to the A cells) passing to a small-amplitude limit attractor (like that in Fig. 9 due to the sources in SA cells), and as the number of SA cells connected increases, the amplitude of the limit cycle increases to become a full size limit cycle of each cell in the net (like those in figures 9 and figure 2. Remarkably the bifurcation parameters give also the structure of the tree in each model, structure which coincides, at least locally, with interdigitations of A and SA cells.

Discussion

There are at least three models of the organization of the SAN . The gradient model [33], [34], [3], the mosaic model [29], and some kind of conciliatory model between the last two [8]. The mosaic model assumes the coexistence of A cells with SA cells within the SAN, whereas the gradient model consider that within the SAN there are only SA cells showing smooth transitional properties. Though immunoflourescence labeling, Dobrzynsky et al. [8] noticed that in the center of the SAN there is not a percentage of A cells as claimed in some papers by the mosaic model defenders [29], but

that contrary to the gradient model, there is a mix of A cells and SA cells in the periphery of the SAN. All this models may be summarized taking into account the equation (1). The three models use $g_{SA-A} = g_{A-SA}$. For gradient model g_1 , to g_4 are matrices with coefficients depending on the position of each cell. For mosaic model g_1 , to g_4 are just constant numbers independent of the cells positions. Most of the actual matrices used modeling mosaic and gradient models are quite simple, for instance in Zhang et al. model [33], the cells are arranged like a chessboard, so that the connection matrices are sum of tridiagonal matrices. One dimensional models (series models) require only one tridiagonal matrix instead of sum of matrices as the model in [34]. In many models the transition between SA center and atrial zone is achieved with only one cell connected in one extreme with a SA cell, and in the other extreme connected to A cells; for instance in Inada et al. model [13], one SA cell is connected with three series of 50 A cells each. Here is where this models are misleading. A series with three branches is not only physiologically improbable, but mathematically wrong since it has only one attractor: the polarized state of the atrial cells. To model appropriately the sink-source dynamics of the periphery of the SAN mathematical models should include an stable limit cycle. Authors in [13], for instance, obtain a limit cycle allowing non experimentally observed conductances of the order of 4000 nS and introducing a gradient in some parameters including conductance between cells.

In the literature some models of the transitional zone between SA and A cells require non experimental conductance values in order to obtain propagation of the AP generated in the SA node. On the contrary, in this paper we obtained models which do not require artificial parameter values to achieve propagation. Our models mimic locally the strand structure (interdigitations) observed and studied in classical papers as [32], and in recent papers as [6]. On the other hand, our models are compatible with mosaic models but may allow the implementation of gradients in some variables as long as this variables do no modify drastically observed conductance values. Mathematically, our successfully conducting AP models may be explained by a supercritical Andronov-Hopf bifurcation associated to a correct source-sink relationship in the transitional zone. Remarkably, the bifurcation parameters of the Andronov-Hopf bifurcation give a geometrical distribution between A and SA cells which is compatible with interdigitating bundles structure of the transitional zone. Hence we conclude that in modeling the cytoarchitecture of the transitional zone between SAN and Atrial zone is essential for smooth propagation of AP to include geometrical arrangements, accordingly with some bifurcation parameters of the dynamical systems theory.

References

1. Adler CP, Costabel U. *Cell number in human heart in atrophy, hypertrophy, and under the influence of cytostatics*. Recent Adv Stud Cardiac Struct Metab. 1975;6:343-55.
2. Agullo-Pascual E., Delmar M., *The “non-canonical” functions of Cx43 in the heart*. J Membr Biol. 2012 August; 245(8): 477-482.
3. Boyett M.R., Honjo H., Kodama I., *The sinoatrial node, a heterogeneous pacemaker structure*. Cardiovascular Research DOI: [http://dx.doi.org/10.1016/S0008-6363\(00\)00135-8](http://dx.doi.org/10.1016/S0008-6363(00)00135-8) 658-687. Vol 47(7): 907-918, 1999.
4. Coppen S. R., Kodama I., et al *Connexin 45, a Major Connexin of the Rabbit Sinoatrial Node, Is Co-expressed with Connexin43 in a restricted Zone at the*

- nodal-Crista Terminalis Border*. The Journal of Histochemistry & Cytochemistry Vol 47(7):907-918, 1999.
5. Courtemanche M., Ramirez R., Nattel S., *Tonic mechanisms underlying human atrial action potential properties: insights from mathematical model*. the American Physiological Society, H301-H321 (1998).
6. Csepe T. A., Zhao J., et al. *Human sinoatrial node structure: 3D microanatomy of sinoatrial conduction pathways*. Progress in Biophysics and Molecular Biology 120(2016) 164-178.
7. Cherry E. M., Hatings, H. M., Evans S. T., *Dynamics of human atrial cell models: Restitution memory, and intracellular calcium dynamics in single cells*. Progress in Biophysics and Molecular Biology 98 (2008) 24-37.
8. Dobrzynski H., Telles J, et al. *Computer Three-Dimensional Reconstruction of the Sinoatrial Node*. Circulation, pp. 846-854 (2005).
9. Colli Franzone P., Pavarino L., *A parallel solver for reaction-diffusion systems in computational electrocardiology*. Mathematical Models and methods in Applied Sciences Vol. 14, No. 6 (2004) 883-911.
10. Colli Franzone P., Guerri L., *Spreading of Excitation in 3-D Models of the Anisotropic Cardiac Tissue. I. Validation of the Eikonal Model*. Mathematical Biosciences 113:145-209 (1993).
11. Colli Franzone P., Guerri L., et al., *Spreading of Excitation in 3-D Models of the Anisotropic Cardiac Tissue. II. Effects of Fiber Architecture and Ventricular Geometry* . Mathematical Biosciences 147:131-171 (1998).
12. Hoyt R. H., Cohen M.L., et al. *Distribution and Three-Dimensional Structure of intercellular Junctions in Canine Myocardium*. Circ Res. 1989; 64: 563-574.
13. Inada, S., Zhang, H. et al. *Importance of Gradient in Membrane Properties and Electrical Coupling in Sinoatrial Node Pacing*. PLOS ONE, April 2014 Vol 9 Issue 4 e94565.
14. Izhikevich, E. M., *Dynamical Systems in Neuroscience, the geometry of excitability and Bursting*. Massachusetts Institute of Technology 2010.
15. Joyner R. W., van Capelle F. J. L., *Propagation Through electrically Coupled Cells. How a Small SA Node Drives a Large Atrium*. Biophys. J. Vol 50 Dec 1986 1157-1164.
16. Lindblad D. S., Murphey C. R., Clark J. W., Giles WR., *A model of the action potential and underlying membrane currents in a rabbit atrial cell*. Am J Physiol. 1996 Oct;271(4 Pt 2):H1666-96.
17. Lugo C. A., Cantalapiedra I. R., Peñaranda A., Hove-Madsen L., Echebarria B. *Are SR Ca content fluctuations or SR refractoriness the key to atrial cardiac alternans?: insights from a human atrial model*. Am J Physiol Heart Circ Physiol. 2014 Jun 1;306(11):H1540-52. doi: 10.1152/ajpheart.00515.2013. Epub 2014 Mar 7.
18. Masson-Pévet, M. A., Bleeker, W. K., et al. *Pacemaker Cell Types in the Rabbit Sinus Node: A correlative Ultrastructural and Electrophysiological Study*. J Mol Cell Cardiol 16, 53-63 (1984).

19. Nygren A., Fiset C., Firek L., Clark J. W., Lindblad D. S., Clark R. B., Giles W. R. *Mathematical Model of an adult Human Atrial Cell. The Role of K^+ Currents in Repolarization.* Circ Res. 1998; 63-81.
20. Oosthoek, P. W., Virágh, S. et al. *Immunohistochemical Delineation of the Conduction System I: The Sinoatrial Node.* Circ Res 1993;73:473-481.
21. Oren, R. V., Clancy, C. E. *Determinants of Heterogeneity, Excitation and Conduction in the Sinoatrial Node: A model Study.* PLOS Computational Biology, December 2010, Vol 6 Issue 12 e1001041.
22. Orthof T., *The mammalian sinoatrial node.* Cardiovascular Drugs and Therapy 1: 573-597, 1988.
23. Panfilov A., Keener J., *Re-entry in three-dimensional Fitzhugh-Nagumo medium with rotational anisotropy.* Physica D 84 (1995) 545-552.
24. Ramirez R. J., Nattel S., Courtemanche M., *Mathematical analysis of canine atrial action potentials: rate, regional factors, and electrical remodeling.* Am J Heart Circ Physiol 279: H1767-H1785, 2000.
25. Severi S. , Fantini M. , Charawi L. A., DiFrancesco D. *An updated computational model of rabbit sinoatrial action potential to investigate the mechanisms of heart rate modulation* J Physiol 590.18 (2012) pp 4483–4499 4483.
26. Shimada T., Kawazato H., et al. *Cytoarchitecture and Intercalated Discs of the working Myocardium and the Conduction System in the Mamalian Heart. The anatomical Record Part A* 280A:940-951 (2004).
27. Spach M., Heidlage J. F., *The Stochastic Nature of Cardiac Propagation at a Microscopic Level.* Circ Res., 76(3): 366-380, Mar 1995.
28. Torre, V. *A theory of Syncchronization of Heart Pace-maker Cells.* J. theor. Biol. (1976), 55-71.
29. Verheijck E., Wessels A., et al., *Distribution of Atrial and Nodal Cells Within the rabbit Sinoatrial Node.* Circulation. 1998; 97: 1623-1631 doi: 10.1161/01.CIR.97.16.1623
30. Verheule, S., van Kempen M. J., Postma, S. et al. *Gap Junctions in the rabbit sinoatrial node.* Am J Physiol Heart Circ Physiol (2001) 280; H2103-2115.
31. Verheule, S., van Kempen M. J. et al. *Characterization of gap junction channels in adult rabbit atrial and ventricular myocardium.* Circ Res 1997(80); 673-681.
32. Winslow, R. L., Jongsma, H. J., *Role of tissue geometry and spatial localization of gap junctions in generation of the pacemaker potential.* Journal of Physiology (1995) 487. P.
33. Zhang H., Holden A. V., Boyett M.R., *Gradient Model Versus Mosaic Model of the Sinoatrial Node* Circulation pp. 584-588 (2000).
34. Zhang H., et al. *Mathematical models of action potentials in the periphery and center of the rabbit sinoatrial node.* Am J Physiol Heart Circ Physiol 279: H397-H421, 2000.